Communication
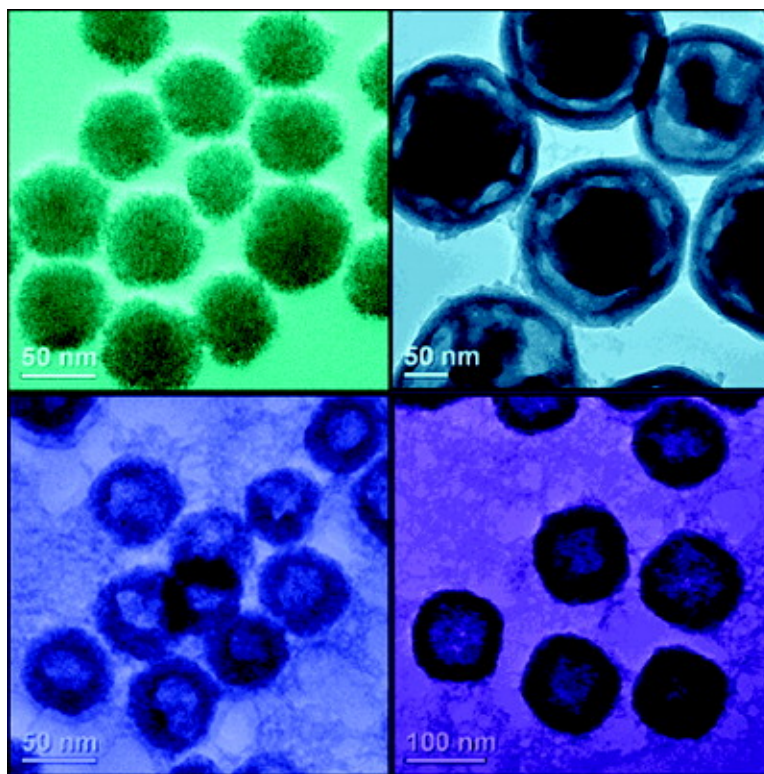
Formation of CeO−ZrO Solid Solution Nanocages with Controllable Structures via Kirkendall Effect

Xin Liang, Xun Wang, Yuan Zhuang, Biao Xu, Simin Kuang, and Yadong Li

More About This Article

Additional resources and features associated with this article are available within the HTML version:

- Supporting Information
- Links to the 6 articles that cite this article, as of the time of this article download
- Access to high resolution figures
- Links to articles and content related to this article
- Copyright permission to reproduce figures and/or text from this article

Formation of CeO$_2$−ZrO$_2$ Solid Solution Nanocages with Controllable Structures via Kirkendall Effect

Xin Liang, Xun Wang,* Yuan Zhuang, Biao Xu, Simin Kuang, and Yadong Li*

Department of Chemistry, Tsinghua University, Beijing, 100084, P. R. China

Received December 9, 2007; E-mail: wangxun@mail.tsinghua.edu.cn; ydli@mail.tsinghua.edu.cn

The solid-solution of ceria and zirconia-containing composites have attracted considerable interests for more than half a century for its far-ranging applications in catalysts, fuel cell, ceramics, gas sensors, solid-state electrolytes, and especially the crucial application as promoters of three-way catalysts (TWC), which are commonly used to reduce the emissions of CO, NO$_x$, and hydrocarbons from automobile exhausts.[1−3] The Ce$_{1−x}$Zr$_x$O$_2$-type solid solution is a key component in these catalysts, due to its redox properties, oxygen storage, and releasing capacity and thermal stability.[4−5] Engineering the nanomaterials to obtain enhanced properties appears as an advancing front in designing and selecting catalysts and catalyst promoters for specific catalytic reactions.[6−7] The CeO$_2$−ZrO$_2$ composites with diameters in nanometer region usually have high specific surface areas and high oxygen storage capacities, which may highly improve the catalytic performance. Till now, there are various synthetic routes for preparation of solid solutions of CeO$_2$−ZrO$_2$, such as coprecipitation, high-temperature calcinations, high-energy mechanical milling, surfactant-assisted approach, micro-emulsion, sol−gel technique, and chemical filing, etc.[8−12] However, both soft aggregation and hard aggregation of CeO$_2$−ZrO$_2$ nanoparticles are the main encumbrances faced by synthetic chemists, and it is hard to define the particle size accurately because of the aggregations, which may bring difficulties in fully addressing fundamental issues in catalytic reactions such as size effects. The morphology monotony is the other main problem that should be addressed. The most common morphology of CeO$_2$−ZrO$_2$ composite is irregular nanoparticles, and subtle fabrication of CeO$_2$−ZrO$_2$ composites with tunable sizes, shapes, and compositions remains as a big challenge.

Herein, monodispersed ceria nanospheres with different shapes were first fabricated via a hydrolysis process in glycol and were used as precursors. Then, zirconium(IV) was added to react with the monodispersed ceria nanospheres in the glycol medium to form CeO$_2$−ZrO$_2$ nanocages with controlled shapes, sizes, and compositions.

Monodispersed ceria colloid nanocrystal clusters with different shapes can be prepared via a hydrolysis process in glycol. The formation process of the nanospheres can be well understood by the reported two-stage growth model, in which nanosized crystalline precursors are nucleated first in supersaturated solution and then the initially formed small particles aggregate into larger secondary particles.[13−15] The obtained products can be well dispersed without deposition for several days in polar solvents, such as water, ethanol, and glycol for there were vast glycol hydroxyl groups attached on the surface of the particles. The water concentration in the reaction system has great influence on the morphology of the obtained ceria. It has been found that nearly cubic ceria clusters have been formed when 4 mL more H$_2$O was added in the origin system. Figure 1 show the typical TEM images of the obtained ceria spherical and nearly cubic ceria clusters with narrow size distribution, respectively.
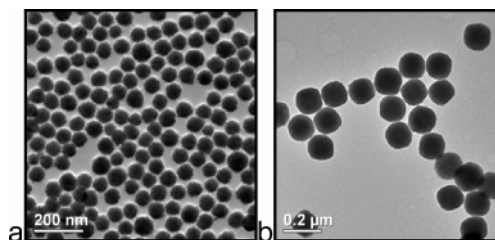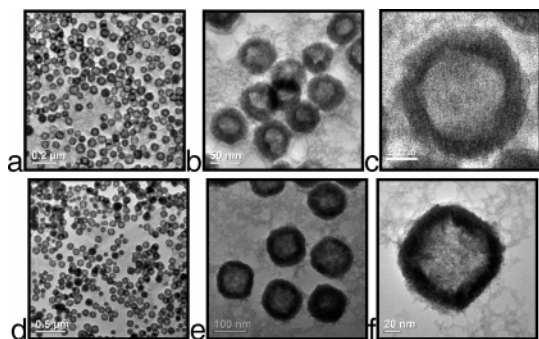

Figure 1. (a) Representative TEM images of nearly monodispersed spherical ceria nanocrystal clusters obtained at low water concentration; (b) representative TEM images of nearly cubic-like ceria nanocrystal clusters obtained at high water concentration.

HRTEM images (SI 2) showed that the big ceria nanosphere was composed of many small nanoparticles, with a size about 4−5 nm. The analysis based on the crystal fringes revealed that the distances between the adjacent crystal fringes in the same direction within different small nanoparticles have the same value, 0.31 nm, which were appointed to the {111} crystal planes of ceria face-centered cubic phase.

XRD patterns of spherical and nearly cubic-like clusters show clusters with different shapes all belonged to the pure phase of ceria face-centered cubic phase. The broadening of the peaks confirmed that monodispersed ceria clusters were composed of primary small particles (Supporting Information, SI 4). The specific surface areas have been confirmed to be 54.0 m^2/g for spherical clusters and 29.8 m^2/g for nearly cubic clusters by BET measurements. This result also supported the secondary structure of the clusters for the measured specific areas are much higher than the calculated value for the single-crystal with identical size.

The secondary structure of the ceria colloid clusters brings some interesting properties. The secondary structures make the ceria clusters with high reactivity and diffusing rates a good template for the formation of a novel hollow structure via the Kirkendall effect. Since Yin and Alivisatos et al. successfully synthesized CoS nanocages via the Kirkendall effect, using the Kirkendall effect to synthesis hollow structures within nanoscale has become a new focus of research.[16−20] The Kirkendall effect declares that each species has its own diffusing rate in a diffusing system.[16] CeO$_{2−x}$ nanotubes have been obtained by the valence transition between Ce^{3+} and Ce^{4+}.[21−22] Herein, the reaction between Zr^{4+} and CeO$_2$ was exploited. Zr^{4+} can readily dope into ceria to form the solid solution of a Ce$_{1−x}$Zr$_x$O$_2$ type. Meanwhile, the diffusing rate of the special secondary nanostructure of our obtained clusters is obviously much faster than that of the single-crystal nanostructure. These two facts implied the possibility of fabricating hollow nanostructures of Ce$_{1−x}$Zr$_x$O$_2$ type via the Kirkendall effect. Therefore, obtained ceria colloid clusters have been exploited as both physical and chemical templates to generate ceria and zirconia composites with well-defined shapes, tunable compositions, narrow size distributions, and hollow interiors via a modified Kirkendall effect.

Figure 2. (a–c) Representative TEM image of spherical Ce−Zr−O nanocages with different magnifications; (d–f) Representative TEM images of nearly cubic-like Ce−Zr−O nanocages with different magnifications.
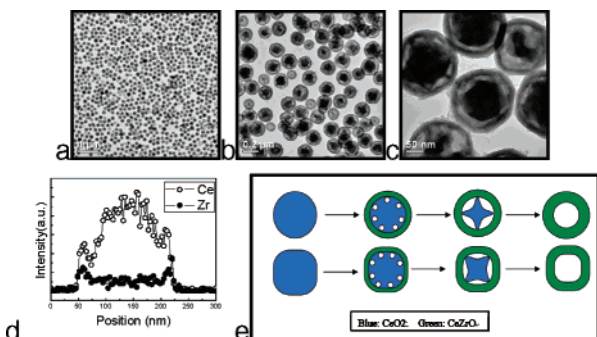
Figure 3. (a–c) Typical TEM images with different magnifications of the hollow core−shell nanostructures obtained by shortening the reaction time; (d) compositional line profile across a single hollow core−shell structure probed by EDS line scanning; (e) the illustration about the formation process of the Ce−Zr−O nanocages based on Kirkendall effect.

A quantity of 0.5 M Zr^{4+} solution was added into the obtained monodispersed ceria clusters according to a molar ratio of 0.3. Then the mixture reacted at 180 °C for several hours. Nanocages with different shapes can be successfully synthesized. Figure 2 showed the spherical and nearly cubic nanocages with narrow size distribution. The shell thickness can be adjusted by controlling the reaction time. (SI 5) The morphologies of the nanocages and the hollow interiors have been decided by the morphology of the ceria templates. When spherical ceria clusters were used as precursors, spherical nanocages have been obtained; whereas cubic nanocages formed when nearly cubic ceria clusters were used as precursors. These materials have high surface areas (182.9 m^2/g for spherical nanocages and 142.0 m^2/g for nearly cubic nanocages), which were favorable for the catalytic performances.

The chemical composition and phase purity of the obtained $Ce_{1−x}Zr_xO_2$ nanocages have been characterized by the X-ray diffraction and energy dispersive spectrometry. XRD patterns of hollow nanospheres and nearly cubic-like nanocages can be appointed to the pure face-centered cubic phase. Corresponding EDS analysis of a single nanocage revealed the molar ratio of Ce and Zr content is similar with the original ratio of reactant. (SI 3)

Figure 3e has shown the illustration about the whole morphology evolution process according to Kirkendall effect.[19−20] On the basis of this mechanism, monodispersed hollow core−shell structures can be obtained by shortening the reaction time. Figure 3 displayed the TEM images of the unique hollow structures with different magnifications. It can be seen that most objects in Figure 3 have a bulk core in the hollow interior. The compositional line profile across a single hollow core−shell structure probed by EDS line scanning (Figure 3d) revealed that the Zr content in the fringe area in much higher than Zr content in center area, which confirmed

that the shell material is $Ce_{1−x}Zr_xO_2$ solid solution and the core material is un-consumption CeO_2.[23] The unique $CeO_2@Ce_{1−x}ZrxO_2$ hollow core−shell structure may bring us novel properties and applications, especially in three-way catalysts.

In summary, spherical and nearly cubic-like monodispersed ceria colloid nanocrystal clusters have been fabricated via a simple hydrolysis process in glycol. Then $Ce_{1−x}Zr_xO_2$ and $CeO_2@Ce_{1−x}Zr_xO_2$ nanocages with different outer and interior morphologies have been prepared using the colloid ceria clusters as both chemical precursors and physical templates by Kirkendall effect. This approach has shown great flexibilities in controlling the sizes, shapes, and compositions of the solid solution. Owing to the penetrability of the shell of these nanocages, different noble metal catalysts may be controlled to deposit inside or outside of these nanostructures, which may serve as novel nanoreactors for environmental catalysis and bring some new opportunities to this old but active research field.

Note Added after ASAP Publication. Experimental details were added to the Supporting Information on February 12, 2008.

Supporting Information Available: HRTEM anlysis of ceria clusters; energy dispersive spectrometry, XRD patterns, HRTEM and FTIR spectrum of the Ce−Zr−O nanocages; TEM images of nanocages with different shell thickness; TEM images of the nanocages formed at different Zr/CeO_2 molar ratio. This material is available free of charge via the Internet at http://pubs.acs.org.

References

(1) Kašpar, J.; Fornasiero, P.; Graziani, M. *Catal. Today* **1999**, *50*, 285.
(2) Steele, B. C. H. *Nature* **1999**, *400*, 619.
(3) Steele, B. C. H.; Heinzel, A. *Nature* **2001**, *414*, 345.
(4) Trovarelli, A. *Catal. Rev. Sci. Eng.* **1996**, *38*, 439.
(5) Liu, G.; Rodriguez, J. A.; Hrbek, J.; Dvorak, J.; Peden, C. H. F. *J. Phys. Chem. B* **2001**, *105*, 7762.
(6) Zhang, F.; Chan, S.-W.; Spanier, J. E.; Apak, E.; Jin, Q.; Robinson, R. D.; Herman, I. P. *Appl. Phys. Lett.* **2002**, *80*, 127.
(7) Rodriguez, J.; Hanson, J. C.; Kim, J.-Y.; Liu, G. *J. Phys. Chem. B* **2003**, *107*, 3535−3543.
(8) Alifanti, M.; Baps, B.; Blangenois, N.; Naud, J.; Grange, P.; Delmon, B. *Chem. Mater.* **2003**, *15*, 395.
(9) Wang, Z. L.; Feng, X. *J. Phys. Chem. B* **2003**, *107*, 13563.
(10) Yuan, Q.; Liu, Q.; Song, W. G.; Feng, W.; Pu, W. L.; Sun, L. D.; Zhang, Y. W.; Yan, C. H. *J. Am. Chem. Soc.* **2007**, *129*, 6698.
(11) Yang, S. W.; Gao, L. *J. Am. Chem. Soc.* **2006**, *128*, 9330.
(12) Carrettin, S.; Concepcion, P.; Corma, A.; Nieto, J. M. L.; Puntes, V. F. A. *Angew. Chem., Int. Ed.* **2004**, *43*, 2538.
(13) Ge, J. P.; Hu, Y. X.; Biasini, M.; Beyermann, W. P.; Yin, Y. D. *Angew. Chem. Int. Ed.* **2007**, *46*, 4342.
(14) Libert, S.; Gorshkov, V.; Goia, D.; Matijevi, E.; Privman, V. *Langmuir* **2003**, *19*, 10679.
(15) Deng, H.; Li, X. L.; Peng, Q.; Wang, X. Chen; J. P.; Li, Y. D. *Angew. Chem., Int. Ed.* **2005**, *44*, 2782.
(16) (a) Yin, Y. D.; Rioux, R. M.; Erdonmez, C. K.; Hughes, S.; Somorjai, G. A.; Alivisatos, A. P. *Science* **2004**, *304*, 711. (b) Yin, Y. D.; Erdonmez, C. K.; Cabot, A.; Hughes, S.; Alivisatos, A. P. *Adv. Funct. Mater.* **2006**, *16*, 1389.
(17) Kim, D.; Park, J.; An, K.; Yang, N.-K.; Park, J.-G.; Hyeon, T. *J. Am. Chem. Soc.* **2007**, *129*, 5812.
(18) Fan, H. J.; Knez, M.; Scholz, R.; Nielsch, K.; Pippel, E.; Hesse, D.; Zacharias, M.; Gösele, U. *Nat. Mater.* **2006**, *5*, 627.
(19) Liu, B.; Zeng, H. C. *J. Am. Chem. Soc.* **2004**, *126*, 16744.
(20) Fan, H. J.; Knez, M.; Scholz, R.; Hesse, D.; Nielsch, K.; Zacharias, M.; Gösele, U. *Nano Lett.* **2004**, *7*, 993.
(21) Han, W-Q.; Wu, L. J.; Zhu, Y. M. *J. Am. Chem. Soc.* **2005**, *127*, 12814.
(22) Zhou, K.; Yang, Z.; Yang, S. *Chem. Mater.* **2007**, *19*, 1215.
(23) Goldberger, J.; He, R. R.; Zhang. Y. F., Lee, S.; Yan, H. F.; Choi, H-J.; Yang, P. D. *Nature* **2003**, *422*, 566.

JA7109629